

# Shadow, deflection angle and quasinormal modes of Born-Infeld charged black holes

Khadije Jafarzade,<sup>1,\*</sup> Mahdi Kord Zangeneh<sup>2,†</sup> and Francisco S. N. Lobo<sup>3,‡</sup>

<sup>1</sup>*Department of Physics, Faculty of Science, University of Mazandaran, Babolsar 47416-95447, Iran*

<sup>2</sup>*Physics Department, Faculty of Science, Shahid Chamran University of Ahvaz, Ahvaz 61357-43135, Iran*

<sup>3</sup>*Instituto de Astrofísica e Ciências do Espaço, Faculdade de Ciências da Universidade de Lisboa, Departamento de Física, Faculdade de Ciências da Universidade de Lisboa,*

*Edifício C8, Campo Grande, P-1749-016, Lisbon, Portugal*

(Dated: December 22, 2024)

In this paper, we consider black holes in four-dimensional Einstein-Gauss-Bonnet (4D EGB) gravity in the presence of Born-Infeld (BI) nonlinear electrodynamics. We study several optical features of these black holes such as the shadow radius, energy emission rate and deflection angle, and analyse the effect of the coupling constants, the electric charge and cosmological constant on the considered optical quantities. Furthermore, we also employ the connection between the shadow radius and quasinormal modes (QNMs) and investigate small scalar perturbations around the black hole solution. We show that the variation of the parameters of the theory provide specific signatures on the optical features of the BI charged black hole solution, thus leading to the possibility of directly testing this 4D EGB black hole model by using astrophysical observations.

## I. INTRODUCTION

Recently, a novel four-dimensional Einstein-Gauss-Bonnet (4D EGB) gravity was proposed by Glavan and Lin [1] by rescaling the Gauss-Bonnet (GB) coupling  $\alpha \rightarrow \alpha/(D-4)$ , and then defining the four-dimensional theory as the limit  $D \rightarrow 4$ , at the level of the field equations. In this manner, the GB term yields a non-trivial contribution to the gravitational dynamics. It has also been discussed whether this regularized theory is reliable [2–9] and several remedies have been suggested to overcome the objections raised [9–12]. It is worthwhile to mention that these theories still hold the spherically symmetric 4D black holes as valid solutions [10, 11]. In fact, the novel 4D EGB theory of gravity has recently attracted much attention in a wide context of black hole physics [13–18], and applications, such as, in black hole shadows [19–22], thermodynamics issues [23, 24], rotating solutions [25–27], stability issues [28–35], gravitational lensing [36], thin accretion disk around 4D EGB black holes [37], causal structure [38, 39], and black hole solutions coupled to nonlinear electrodynamics [40–44].

Motivated by recent astrophysical observations, namely, the first image of a supermassive black hole candidate in the center of M87 galaxy captured by the Event Horizon Telescope project [45, 46], we are interested in performing an in-depth analysis of the optical features of black hole solutions. More specifically, we consider the solution obtained in 4D EGB gravity minimally coupled to Born-Infeld (BI) electrodynamics in the presence of a negative cosmological constant, provided in [43]. In fact, BI electrodynamics is a well-known nonlinear electromagnetic theory, proposed by Born and Infeld in 1934

[47], in order to regularize the ultraviolet divergent self-energy of a point-like charge in classical dynamics. Moreover, it was shown later that this nonlinear theory may come from the low energy limit of open superstring theory [48–50]. In addition, experiments of photon-photon interaction have proposed a nonlinear model for electrodynamics in vacuum [51–55]. In the context of 4D EGB gravity, several generalized solutions were obtained in the literature such as generalized Reissner-Nordstrom black hole with a Maxwell electric field coupling to the 4D EGB gravity [13], Bardeen-like [15] and Hayward-like [16] black holes by interacting the new gravitational theory with nonlinear electrodynamics, and AdS black holes in the novel 4D EGB gravity coupled to exponential nonlinear electrodynamics [40–42]. Thus, in this work, we specifically analyse the shadow geometrical shape, the energy emission rate, the deflection angle and quasinormal modes in the BI charged black hole solution obtained in [43]. The behavior of photon orbits around black holes in the presence of a variety of nonlinear electrodynamics have also been studied in [56, 57].

This paper is organised in the following manner: In section II, we present the action, the field equations, and the specific black hole solution of 4D EGB gravity minimally coupled to BI electrodynamics in the presence of a negative cosmological constant. In section III, we consider the motion of a free photon in the black hole background, and write out the specific condition for a circular null geodesic. Then, we analyse the photon sphere radius by varying the black hole parameters in subsection. We also consider the radius of the shadow and examine the effect of the model's parameters and analyse the energy emission rate. In section IV, we study the connection between the radius of the shadow and quasinormal modes and consider small perturbations around the black holes. In section V, we consider the light deflection around the black hole solution. Finally, in section VI, we conclude by summarizing and discussing our results.

---

\* khadije.jafarzade@gmail.com

† mkzangeneh@scu.ac.ir

‡ fslobo@fc.ul.pt

## II. ACTION AND BLACK HOLE SOLUTION

The action of  $D$ -dimensional EGB gravity minimally coupled to Born-Infeld (BI) electrodynamics in the presence of a negative cosmological constant is given by [43]

$$S = \frac{1}{16\pi} \int d^D x \sqrt{-g} \left( R - 2\Lambda + \frac{\alpha}{D-4} \mathcal{G} + \mathcal{L}_{BI} \right), \quad (1)$$

where  $\mathcal{G} = R^2 - 4R_{\mu\nu}R^{\mu\nu} + R_{\mu\nu\rho\sigma}R^{\mu\nu\rho\sigma}$  is the GB term,  $\Lambda = -(D-1)(D-2)/2l^2$  is a negative cosmological constant, and  $\mathcal{L}_{BI}$  is the Lagrangian of BI electrodynamics provided by

$$\mathcal{L}_{BI} = 4\beta^2 \left( 1 - \sqrt{1 + \frac{2F}{\beta^2}} \right). \quad (2)$$

with  $F = \frac{1}{4}F_{\mu\nu}F^{\mu\nu}$ , where  $F_{\mu\nu} = \partial_\mu A_\nu - \partial_\nu A_\mu$  and  $A_\mu$  is the potential, and here  $\beta > 0$  denotes the BI parameter which is the maximum of the electromagnetic field strength.

Varying the action with respect to the metric,  $g_{\mu\nu}$ , and gauge field,  $A_\mu$ , provides the following equations of motion

$$G_{\mu\nu} + \Lambda g_{\mu\nu} + \frac{\alpha}{D-4} \left( 2RR_{\mu\nu} + 2R_\mu^{\rho\sigma\lambda} R_{\nu\rho\sigma\lambda} - 4R_{\mu\lambda}R_\nu^\lambda - 4R^{\rho\sigma} R_{\mu\rho\nu\sigma} - \frac{1}{2}g_{\mu\nu}\mathcal{G} \right) \quad (3)$$

$$+ \left( \frac{2F_{\mu\lambda}F_\nu^\lambda}{\sqrt{1 + 2F/\beta^2}} - \frac{1}{2}g_{\mu\nu}\mathcal{L}_{BI} \right) = 0, \quad (4)$$

and

$$\partial_\mu \left( \frac{\sqrt{-g}F^{\mu\nu}}{\sqrt{1 + 2F/\beta^2}} \right) = 0, \quad (5)$$

respectively.

Consider the following static and spherically symmetric line element

$$ds^2 = -f(r)e^{-2g(r)}dt^2 + \frac{dr^2}{f(r)} + r^2 d\Omega_{D-2}^2, \quad (6)$$

where  $d\Omega_{D-2}^2$  is the  $(D-2)$ -dimensional unit sphere. In  $D = 4$ , the metric functions are given by  $g(r)$  and [43]

$$f(r) = 1 + \frac{r^2}{2\alpha} \left\{ 1 \pm \left[ 1 + 4\alpha \left( \frac{2M}{r^3} - \frac{1}{l^2} - \frac{2\beta^2}{3} \left( 1 - \sqrt{1 + \frac{Q^2}{\beta^2 r^4}} \right) - \frac{4Q}{3r^3} \Phi(r) \right) \right]^{\frac{1}{2}} \right\}. \quad (7)$$

where  $Q$  is the electric charge and  $\Phi(r)$  is defined as

$$\Phi(r) = \frac{Q}{r} {}_2F_1 \left( \frac{1}{4}, \frac{1}{2}, \frac{5}{4}, -\frac{Q^2}{\beta^2 r^4} \right), \quad (8)$$

and  ${}_2F_1$  is the hypergeometric function.

Equation (7) corresponds to two branches of solutions depending on the choice of the sign. It can be shown that the positive-sign branch reduces to a RN-AdS solution with a negative gravitational mass and imaginary charge, and only the negative-sign branch recovers the proper RN-AdS limit (we refer the reader to Ref. [43] for more details). Thus, since only negative branch leads to a physically meaningful solution, we will limit our discussions to this branch of the solution.

## III. NULL GEODESICS AND PHOTON SPHERE

In this section, we analyse the motion of a free photon in the black hole background (7). Due to the spherical symmetry of the spacetime, we consider that the motion is limited to the equatorial plane  $\theta = \pi/2$ , without a significant loss of generality. Thus, the Lagrangian for a photon can be expressed as

$$2\mathcal{L} = -f(r)\dot{t}^2 + \frac{\dot{r}^2}{f(r)} + r^2\dot{\phi}^2, \quad (9)$$

where the overdot denotes a derivative with respect to the affine parameter. Taking into account Eq. (9), the equations of motion are given by

$$\dot{t} = -\frac{p_t}{f(r)}, \quad \dot{r} = p_r f(r), \quad \dot{\phi} = \frac{p_\phi}{r^2}, \quad (10)$$

where  $p$  is the generalized momentum defined by  $p_\mu = \partial\mathcal{L}/\partial\dot{x}^\mu = g_{\mu\nu}\dot{x}^\nu$ .

The Hamiltonian for this system reads

$$H = \frac{1}{2}g^{\mu\nu}p_\mu p_\nu = \frac{1}{2} \left[ -\frac{p_t^2}{f(r)} + f(r)p_r^2 + \frac{p_\phi^2}{r^2} \right] = 0. \quad (11)$$

Since the Hamiltonian is independent of the coordinates  $t$  and  $\phi$ , one can consider  $p_t \equiv -E$  and  $p_\phi \equiv L$  as constants of motion, where  $E$  and  $L$  are physically interpreted as the energy and angular momentum of the photon; note that  $p_r$  is the radial momentum. Using the equations of motion and these two conserved quantities, one can rewrite the null geodesic equation as follows

$$\dot{r}^2 + V_{\text{eff}}(r) = 0, \quad (12)$$

where the effective potential is

$$V_{\text{eff}}(r) = f(r) \left[ \frac{L^2}{r^2} - \frac{E^2}{f(r)} \right]. \quad (13)$$

For a circular null geodesic, the effective potential satisfies the following conditions, simultaneously

$$V_{\text{eff}}(r)|_{r=r_p} = 0, \quad \left. \frac{\partial V_{\text{eff}}(r)}{\partial r} \right|_{r=r_p} = 0. \quad (14)$$

The conditions (14) determine the photon sphere radius ( $r_p$ ) and the critical angular momentum of the photon sphere ( $L_p$ ). Note that the photon orbits are unstable

and are determined by the condition  $\partial^2 V_{\text{eff}}(r)/\partial r^2 < 0$ . The second condition of Eq. (14) yields the following expression

$$\begin{aligned} & \frac{4Q^2}{3} \left( 2\beta^2 r_p^4 - \frac{Q^2}{5} \right) {}_2F_1 \left( \frac{1}{4}, \frac{1}{2}, \frac{5}{4}, -\frac{Q^2}{\beta^2 r_p^4} \right) \\ & + \beta^2 r_p^6 \left\{ \left[ 1 + 4\alpha \left( \frac{2M}{r_p^3} + \frac{\Lambda}{3} - \frac{2\beta^2}{3} \left( 1 - \sqrt{1 + \frac{Q^2}{\beta^2 r_p^4}} \right) \right) \right]^{\frac{1}{2}} - \frac{3M}{r_p} \right\} = 0, \quad (15) \end{aligned}$$

which we solve numerically to obtain the radius of photon sphere. The event horizon ( $r_e$ ) and photon sphere radius ( $r_p$ ) are listed in Table I, by varying several of the black hole parameters. We note that increasing the electric charge, and the GB and BI parameters leads to a decrease in the event horizon and photon sphere radius. However, the BI parameter does not play a significant role in this case. The effect of cosmological constant is slightly different, as increasing this parameter from  $-0.15$  to  $-0.01$  results in a decrease of the photon sphere radius and an increase of the event horizon. A remarkable point regarding the GB parameter is that its increasing leads to an imaginary value for the event horizon, which is physically meaningless. This shows that specific constraints should be imposed on this parameter.

As a next step in the analysis, we consider the radius of the shadow and examine the effect of the model's parameters. From the definition of the shadow radius [58], the size of black hole shadow can be expressed in celestial coordinates ( $x, y$ ) as

$$r_s = \sqrt{x^2 + y^2} = \frac{L_p}{E} = \frac{r_p}{\sqrt{f(r_p)}}. \quad (16)$$

Thus, using Eq. (16) and the listed values of Table I, we explore the shadow size of this solution. To inspect the influence of the black hole parameters on the shadow geometric circular shape, we plot Fig. 1. Evidently, the electric charge decreases the shadow size for fixed values of  $\alpha$ ,  $\beta$  and  $\Lambda$  (see Fig. 1(a)). Taking into account Figs. 1(b) and 1(e), we verify that the GB and BI parameters have a decreasing effect on the shadow radius similar to the electric charge. However, the variation of the BI parameter  $\beta$  does not affect the shadow size significantly. Figure 1(c) depicts the impact of the cosmological constant on the size of the shadow. As we see, unlike the previous parameters, the cosmological constant increases the shadow radius and has a notable effect on it.

It has been known that the black hole shadow corresponds to its high energy absorption cross section for a distant observer. Indeed, the absorption cross section oscillates near to a limiting constant value  $\sigma_{\text{lim}}$  for a spherically symmetric black hole. According to [59–61],  $\sigma_{\text{lim}}$  was found to be equal to the area of the photon sphere ( $\sigma_{\text{lim}} \approx \pi r_s^2$ ). Since the shadow measures the optical

appearance of a black hole, it can be equal to the limiting constant value of the high-energy absorption cross section. The energy emission rate is given by

$$\frac{d^2 E(\omega)}{dt d\omega} = \frac{2\pi^3 \omega^3 r_s^2}{e^{\frac{\omega}{T}} - 1}, \quad (17)$$

where  $\omega$  and  $T$  are, respectively, the emission frequency and Hawking temperature. For the present solution, the Hawking temperature is obtained as

$$T = \frac{1}{4\pi r_e} \left[ \frac{-\Lambda r_e^4 - 3\alpha + 2\beta^2 r_e^4 \left( 1 - \sqrt{1 + \frac{Q^2}{\beta^2 r_e^4}} \right)}{r_e^2 + 2\alpha} + 1 \right]. \quad (18)$$

Figure 2 depicts the behavior of the BH parameters on the energy emission. As it is transparent, there exists a peak of the energy emission rate for the black hole. As the BH parameters increase, the peak decreases and shifts to the low frequency. From Fig. 2(a), we verify that the electric charge decreases the energy emission, so that when the black hole is located in a more powerful electric field, the evaporation process would be slower. Regarding the effects of the GB and BI parameters, we see from Figs. 2(b) and 2(c), that increasing these two parameters results in the decrease of the energy emission. In fact, decreasing the coupling constants implies a fast emission of particles. But as in the shadow case, the effect of  $\beta$  is negligible. Figure 2(d) displays the decreasing contribution of the cosmological constant on the emission rate which shows that the black hole should be located in a lower curvature background in order to have a faster evaporation. The figure also shows that the variation of cosmological constant has a stronger effect on the radiation rate than other parameters.

#### IV. CONNECTION BETWEEN SHADOW RADIUS AND QUASINORMAL MODES

Quasinormal modes (QNMs) are characteristic frequencies with a nonvanishing imaginary part, which encode important information related to the stability of the black hole under small perturbations. These frequencies depend on the details of the geometry and the type of the perturbation, but not on the initial conditions. To study these modes, an outgoing boundary condition should be imposed at infinity and an ingoing boundary condition at the horizon. In general, QNMs are characterized by complex numbers,  $\omega = \omega_R + i\omega_I$ . The sign of the imaginary part determines if the mode is stable or unstable. For positive  $\omega_I$  (exponential growth), the mode is unstable, whereas negativity represents stable modes. In fact, it was shown that the real and imaginary parts of QNMs in the eikonal limit are, respectively, related to the angular velocity and Lyapunov exponent of unstable circular null geodesics [62]. Such a connection was investigated between QNMs and gravitational lensing [63].

TABLE I. The event horizon and photon sphere radius for the variation of the electric charge,  $Q$ , the BI parameter,  $\beta$ , the GB parameter,  $\alpha$ , and the cosmological constant,  $\Lambda$ , for  $M = 1$ .

$Q$	0.1	0.3	0.6	0.9
$r_e(\alpha = \beta = 0.2, \Lambda = -0.02)$	1.84	1.80	1.63	1.30
$r_p(\alpha = \beta = 0.2, \Lambda = -0.02)$	2.91	2.85	2.64	2.18
$\alpha$	0.2	0.5	0.8	0.9
$r_e(Q = \beta = 0.2, \Lambda = -0.02)$	1.83	1.64	1.37	$0.98 + 0.2I$
$r_p(Q = \beta = 0.2, \Lambda = -0.02)$	2.89	2.73	2.54	2.46
$\beta$	0.05	0.1	0.15	0.25
$r_e(Q = \alpha = 0.2, \Lambda = -0.02)$	1.8291	1.8283	1.8281	1.8280
$r_p(Q = \alpha = 0.2, \Lambda = -0.02)$	2.8774	2.8762	2.8760	2.8759
$\Lambda$	-0.01	-0.06	-0.1	-0.15
$r_e(\alpha = \beta = Q = 0.2)$	1.85	1.76	1.70	1.63
$r_p(\alpha = \beta = Q = 0.2)$	2.88	2.90	2.92	2.94

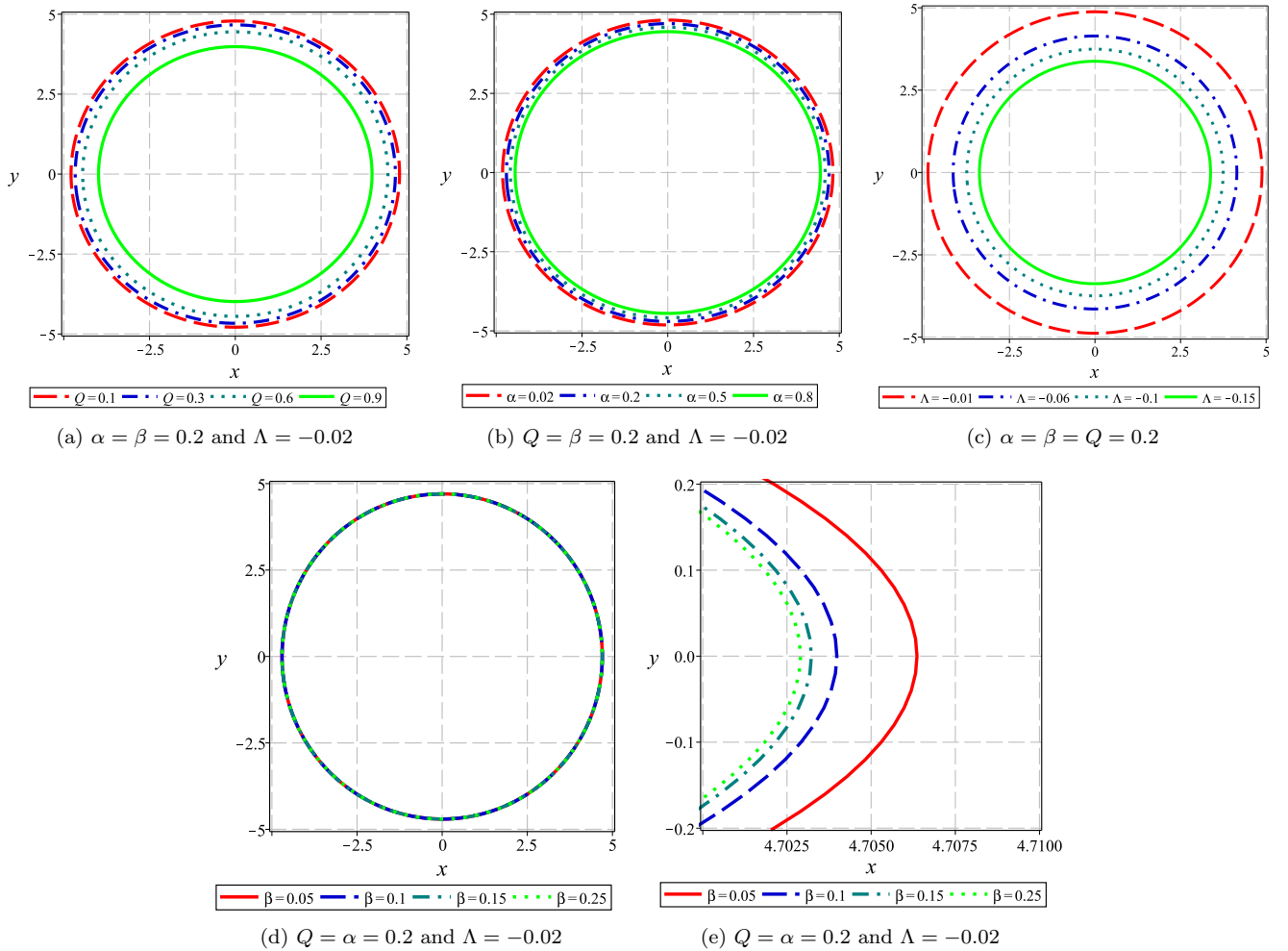


FIG. 1. The plots depict the black hole shadow in the celestial plane ( $x - y$ ) for  $M = 1$ . See the text for more details.

Recently, it has been suggested that the real part of QNMs in the eikonal limit can be connected to the radius of the black hole shadow [64, 65]. Such a correspondence

has been applied to different black holes [66–68]. Here, we employ this idea and study the QNMs for the black hole solution presented by the metric function given in Eq.

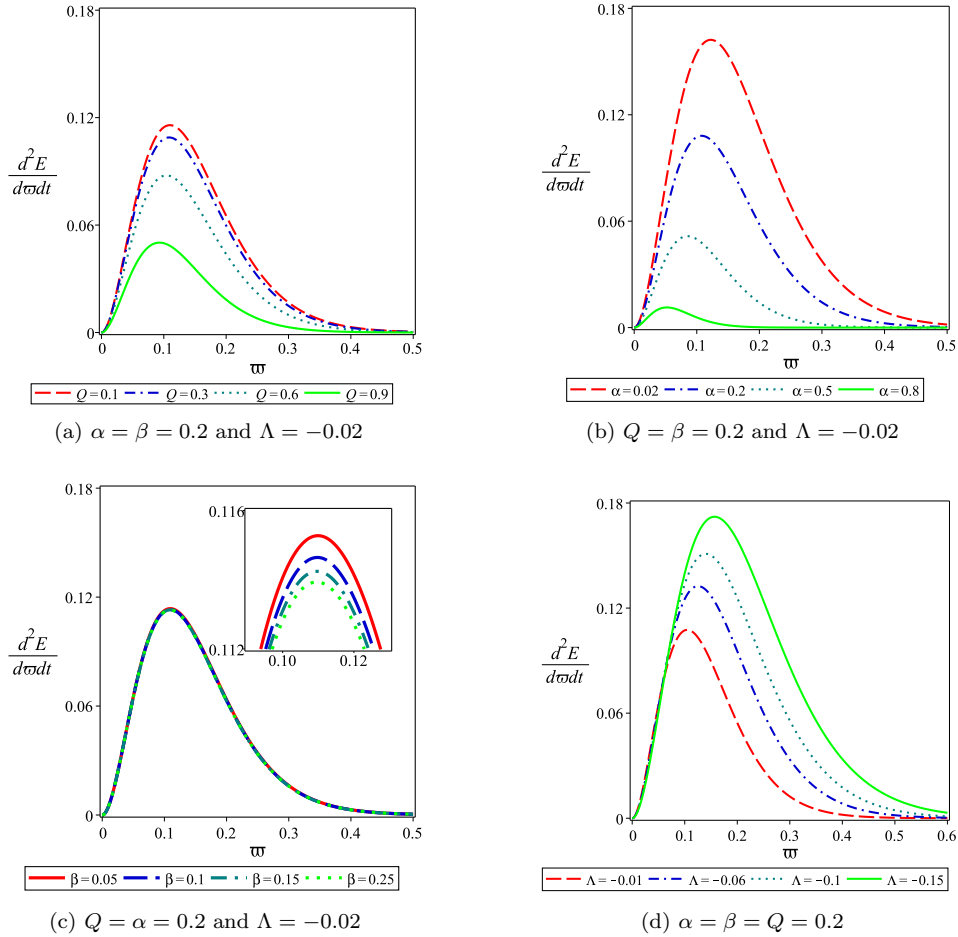


FIG. 2. The energy emission rates for the corresponding black hole, with  $M = 1$ , and different values of  $Q$ ,  $\beta$ ,  $\alpha$  and  $\Lambda$ . See the text for details.

(7). According to this correspondence, the quasinormal frequency  $\omega$  can be calculated with the property of the photon sphere as

$$\omega = L\Omega - i \left( n + \frac{1}{2} \right) |\lambda|. \quad (19)$$

where  $n$  and  $L$  are the overtone number and the angular momentum of the perturbation, respectively. The quantities  $\Omega$  and  $\lambda$  are the angular velocity and Lyapunov exponent of the photon sphere, which can be obtained as

$$\Omega = \frac{\sqrt{f(r_p)}}{r_p} = \frac{1}{L_p}, \quad (20)$$

$$\lambda = \frac{\sqrt{2f(r_p) - r_p^2 f''}}{\sqrt{2}L_p}. \quad (21)$$

From Eq. (19), evidently the real part of the modes is proportional to the angular degree, whereas the imaginary part depends on the overtone number only. Using

Eqs. (19), (20) and (21), we can investigate how the black hole parameters affect quasinormal frequencies. These effects are depicted in Fig. 3, where the spectrum obtained exhibits the following features:

- The real (imaginary) part of the quasinormal frequencies exhibits an increasing (decreasing) behavior for increasing  $\alpha$ . This shows that the scalar field perturbations around a black hole with a stronger GB coupling oscillates with more energy and decays slower.
- According to Figs. 3(a) and 3(b), the electric charge increases (decreases) the real (imaginary) value of the QNM frequency. This indicates that the scalar field perturbations in the presence of electric charge oscillate faster and decay slower as compared to neutral black holes.
- From Figs. 3(c) and 3(d), we verify that the effect of the BI parameter is similar to the GB parameter, but unlike the GB coupling constant, its effect is negligible.

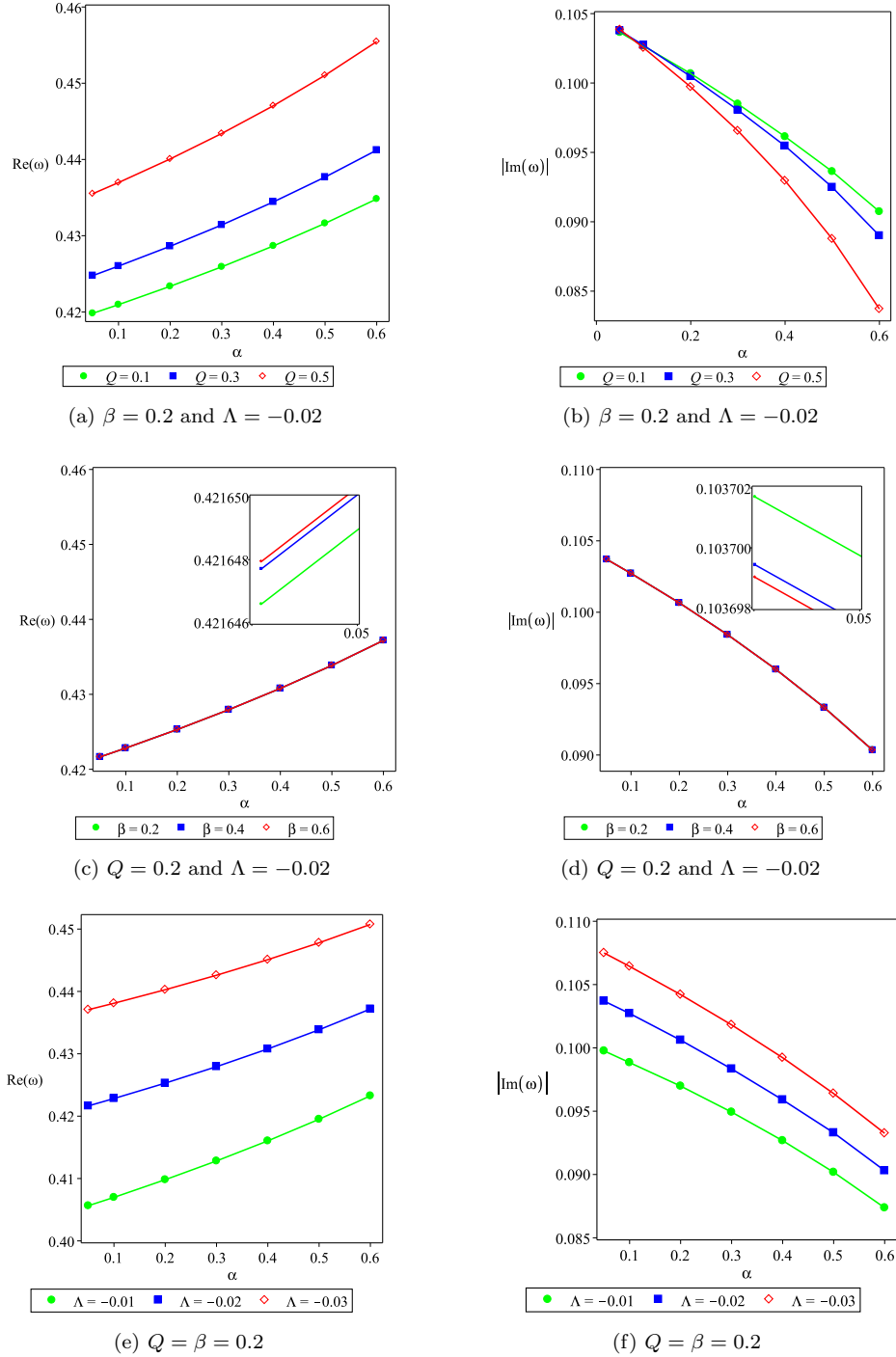


FIG. 3. The behavior of  $Re(\omega)$  and  $Im(\omega)$  with respect to the GB parameter for  $M = 1$ ,  $n = 0$ ,  $L = 2$  and different values of  $Q$  (Figs. 3(a) and 3(b)),  $\beta$  (Figs. 3(c) and 3(d)) and  $\Lambda$  (Figs. 3(e) and 3(f)). See the text for more details.

- Both  $Re(\omega)$  and  $Im(\omega)$  decrease by increasing  $\Lambda$ , which is transparent from Figs. 3(e) and 3(f). This implies that the existence of a higher curvature background restrains the oscillation amplitude of the scalar field, even though it could decay slower.

## V. DEFLECTION ANGLE USING NULL GEODESICS

In this section, we study the light deflection around the black hole solution (7). Employing the null geodesics method [69–72], one can determine the total deflection  $\Theta$

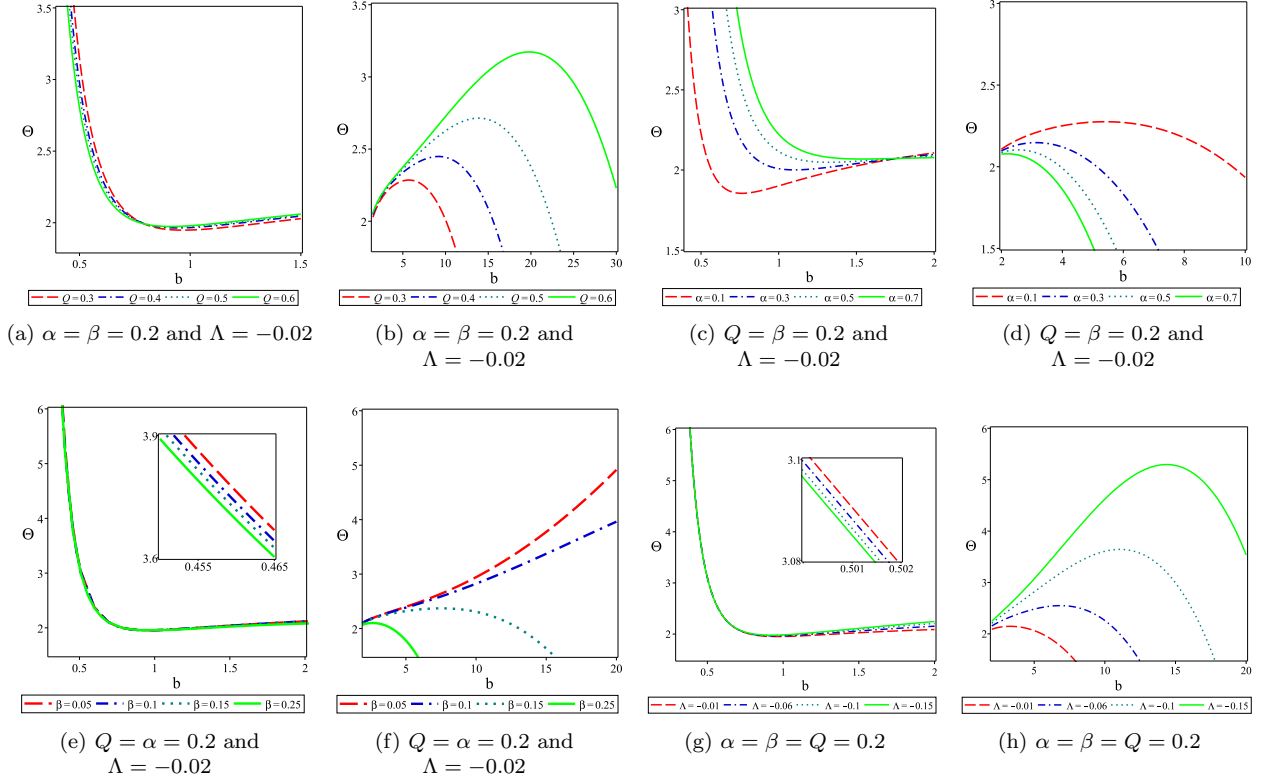


FIG. 4. The behavior of  $\Theta$  with respect to the impact parameter  $b$  for  $M = 1$  and different values of  $Q$ ,  $\beta$ ,  $\alpha$  and  $\Lambda$ . See the text for more details.

by the following relation

$$\Theta = 2 \int_b^\infty \left| \frac{d\phi}{dr} \right| dr - \pi, \quad (22)$$

where  $b$  is the impact parameter, defined as  $b \equiv L/E$ . Using Eq. (22), the deflection angle is obtained as

$$\begin{aligned} \Theta = & \frac{M\alpha(24Mb + 7Q^2)}{42b^5} + \frac{(2\alpha\Lambda - 3)(2Q^2 + 15Mb)}{90b^2} \\ & - \frac{2b^2\beta^2(2\alpha\Lambda - 3)}{27} {}_2F_1\left(-\frac{3}{4}, -\frac{1}{2}, \frac{5}{4}, -\frac{Q^2}{\beta^2b^4}\right) \\ & - \frac{2\alpha b^2\beta^4(5Q^2 + 24Mb)}{189Q^2} {}_2F_1\left(-\frac{7}{4}, -\frac{3}{2}, -\frac{3}{4}, -\frac{Q^2}{\beta^2b^4}\right) \\ & + \frac{7}{3} + \frac{\Lambda b^2(\alpha\Lambda - 3)}{9} + \frac{2\beta^2}{27b^2} [(2\alpha Q^2 + 12\alpha Mb \\ & + b^4(2\alpha\Lambda - 3))] {}_2F_1\left(-\frac{3}{4}, -\frac{1}{2}, \frac{1}{4}, -\frac{Q^2}{\beta^2b^4}\right). \end{aligned} \quad (23)$$

Figure 4 depicts the impact of the black hole parameters on the deflection angle. More specifically, Figs. 4(a) and 4(b) illustrate the effect of electric charge on  $\Theta$ . One verifies that  $\Theta$  is a decreasing (an increasing) function of  $Q$  for small (large) values of the impact parameter. Figures 4(c) and 4(d) indicate the behavior of  $\Theta$  by varying the GB parameter. As we see, for small values of  $b$ , the effect of  $\alpha$  is to increase the deflection angle, whereas for

large  $b$ , its effect is to decrease  $\Theta$ . This shows that the effect of  $Q$  and  $\alpha$  on the deflection angle is opposed to each other. Now, analysing Figs. 4(e) and 4(f), we verify that for all values of the impact parameter, increasing the BI parameter leads to the decreasing of  $\Theta$ . Regarding the cosmological constant effect, we see from Figs. 4(g) and 4(h), that its effect is similar to that of the GB parameter. Using Fig. 4, one can also analyze the behavior of  $\Theta$  by varying the impact parameter. We verify that for small and large values of  $b$ , the deflection angle is a decreasing function of  $b$ , whereas for intermediate values, it is an increasing function; except for low values of  $\beta$ , where the increasing behavior is observed for large values of  $b$  as well (see dashed line in Fig. 4(f)).

## VI. SUMMARY AND CONCLUSION

Motivated by interesting properties of black hole solutions in the recently proposed regularized 4D EGB theory of gravity, we considered Born-Infeld black holes and studied their dynamic features including the shadow size, energy emission rate, quasinormal modes and deflection angle. We first investigated the shadow behavior and photon sphere and examined how the black hole parameters affect them. The results showed that the GB parameter decrease both the photon sphere radius and shadow size, albeit, these quantities are not that sensitive to this

parameter. Studying the effect of electric charge, we noticed that its effect was similar to that of GB coupling constant. However, the effect of the cosmological constant differs. Although it decreases the photon sphere radius, it has an increasing effect on the shadow size. Then, we performed an investigation regarding the energy emission rate and analyzed the effective roles of these parameters on this optical quantity. We found that all these parameters have a decreasing contribution on the emission rate, namely, the emission of particles around the black hole decreases by increasing these parameters. This revealed the fact that such black holes have a longer lifetime if they are located in a background with higher curvature or in a stronger electric field.

Furthermore, we employed the connection between the radius of the shadow and quasinormal modes and studied small perturbations around the black holes. We found that: i) As the coupling constants increase the real part (absolute value of the imaginary part) of the quasinormal frequencies increases (decreases). This means that QNMs oscillate faster and decay slower around the black holes with powerful coupling. ii) The effect of the cosmological constant is to decrease both real and imaginary parts of the QNMs. In other words, scalar perturbations have less energy for oscillation and decay slower in a higher curvature background. iii) The real (imaginary) part of QNM is an increasing (decreasing) function of the electric charge. In fact, the scalar field perturbations in the presence of electric charge oscillate faster and decay more slowly compared to neutral black holes.

Finally, we presented a study in the context of the gravitational lensing of light around these black holes. De-

pending on the choice of the BH parameters, we observed different behaviors. For small and large values of  $b$ , the deflection angle is a decreasing function of  $b$ , whereas for intermediate values, it is an increasing function. Relative to the impact of electric charge, we found that its effect is dependent on the values of the impact parameter, such that for small values of  $b$ ,  $\Theta$  is a decreasing function of  $Q$ , however, for large values, the effect of  $Q$  is opposite. We also found that the effects of the GB parameter and the cosmological constant on the deflection angle are opposed to that of the electric charge. Regarding the influence of BI parameter, it had a decreasing effect for all values of  $b$ , although quite insignificant.

Here, we studied the optical features of the black hole solution in a modified gravity. There are other interesting solutions such as charged accelerating AdS black holes in  $f(R)$  gravity [73], black bounce solutions [74] and regular black holes with an asymptotically Minkowski core [75] which we are currently studying. The results will appear elsewhere.

## ACKNOWLEDGMENTS

MKZ would like to thank Shahid Chamran University of Ahvaz, Iran for supporting this work. FSNL acknowledges support from the Fundação para a Ciência e a Tecnologia (FCT) Scientific Employment Stimulus contract with reference CEECIND/04057/2017. FSNL also thanks funding from the FCT research grants No. UID/FIS/04434/2020, No. PTDC/FIS-OUT/29048/2017 and No. CERN/FIS-PAR/0037/2019.

- 
- [1] D. Glavan and C. Lin, Einstein–Gauss–Bonnet Gravity in Four–Dimensional Space–time, *Phys. Rev. Lett.* **124**, 081301 (2020), [[arXiv:1905.03601](#)].
  - [2] W. Ai, A note on the novel 4D Einstein–Gauss–Bonnet gravity, [arXiv:2004.02858](#).
  - [3] F. Shu, Vacua in novel 4D Einstein–Gauss–Bonnet Gravity: pathology and instability?, [arXiv:2004.09339](#).
  - [4] M. Gurses, T. C. Sisman and B. Tekin, Is there a novel Einstein–Gauss–Bonnet theory in four dimensions?, *Eur. Phys. J. C* **80**, 647 (2020), [[arXiv:2004.03390](#)].
  - [5] S. Mahapatra, A note on the total action of 4D Gauss–Bonnet theory, [arXiv:2004.09214](#).
  - [6] J. Arrechea, A. Delhom and A. Jiménez-Cano, Yet another comment on four–dimensional Einstein–Gauss–Bonnet gravity, [arXiv:2004.12998](#).
  - [7] M. Gurses, T. C. Sisman and B. Tekin, Comment on “Einstein–Gauss–Bonnet Gravity in Four–Dimensional Space–Time”, *Phys. Rev. Lett.* **125**, 149001 (2020), [[arXiv:2009.13508](#)].
  - [8] J. Arrechea, A. Delhom and A. Jiménez-Cano, Comment on “Einstein–Gauss–Bonnet Gravity in Four–Dimensional Space–time”, *Phys. Rev. Lett.* **125**, 149002 (2020), [[arXiv:2009.10715](#)].
  - [9] R. A. Hennigar, D. Kubiznak, R. B. Mann and C. Pollack, On Taking the  $D \rightarrow 4$  limit of Gauss–Bonnet Gravity: Theory and Solutions, *JHEP* **07**, 027 (2020), [[arXiv:2004.09472](#)].
  - [10] A. Casalino, A. Colleaux, M. Rinaldi and S. Vicentini, Regularized Lovelock gravity, [arXiv:2003.07068](#).
  - [11] H. Lu and Y. Pang, Horndeski Gravity as  $D \rightarrow 4$  Limit of Gauss–Bonnet, *Phys. Lett. B* **809**, 135717 (2020), [[arXiv:2003.11552](#)].
  - [12] T. Kobayashi, Effective scalar-tensor description of regularized Lovelock gravity in four dimensions, [arXiv:2003.12771](#).
  - [13] P. G. S. Fernandes, Charged Black Holes in AdS Spaces in 4D Einstein Gauss–Bonnet Gravity, *Phys. Lett. B* **805**, 135468 (2020), [[arXiv:2003.05491](#)].
  - [14] R. A. Konoplya and A. Zhidenko, Black holes in the four-dimensional Einstein–Lovelock gravity, *Phys. Rev. D* **101**, 084038 (2020), [[arXiv:2003.07788](#)].
  - [15] A. Kumar and R. Kumar, Bardeen black holes in the novel 4D Einstein–Gauss–Bonnet gravity, [arXiv:2003.13104](#).
  - [16] A. Kumar and S. G. Ghosh, Hayward black holes in the novel 4D Einstein–Gauss–Bonnet gravity,

- [arXiv:2004.01131](#).
- [17] Y. P. Zhang, S. W. Wei and Y. X. Liu, Spinning test particle in four-dimensional Einstein-Gauss-Bonnet Black Hole, *Universe* **6**, 103 (2020), [[arXiv:2003.10960](#)].
- [18] S. Shaymatov, J. Vrba, D. Malafarina, B. Ahmedov and Z. Stuchlík, Charged particle and epicyclic motions around 4D Einstein-Gauss-Bonnet black hole immersed in an external magnetic field, *Phys. Dark Univ.* **30**, 100648 (2020), [[arXiv:2005.12410](#)].
- [19] R. A. Konoplya and A. F. Zinhailo, Quasinormal modes, stability and shadows of a black hole in the novel 4D Einstein-Gauss-Bonnet gravity, [arXiv:2003.01188](#).
- [20] M. Guo and P. C. Li, Innermost stable circular orbit and shadow of the 4D Einstein-Gauss-Bonnet black hole, *Eur. Phys. J. C* **80**, 588 (2020), [[arXiv:2003.02523](#)].
- [21] B. Eslam Panah, K. Jafarzade and S. H. Hendi, Charged 4D Einstein-Gauss-Bonnet-AdS Black Holes: Shadow, Energy Emission, Deflection Angle and Heat Engine, [arXiv:2004.04058](#).
- [22] X. X. Zeng, H. Q. Zhang and H. Zhang, Shadows and photon spheres with spherical accretions in the four-dimensional Gauss-Bonnet black hole, *Eur. Phys. J. C* **80**, 872 (2020), [[arXiv:2004.12074](#)].
- [23] K. Hegde, A. Naveena Kumara, C. L. A. Rizwan, A. K. M. and M. S. Ali, Thermodynamics, Phase Transition and Joule Thomson Expansion of novel 4-D Gauss Bonnet AdS Black Hole, [arXiv:2003.08778](#).
- [24] D. V. Singh and S. Siwach, Thermodynamics and P-v criticality of Bardeen-AdS Black Hole in 4D Einstein-Gauss-Bonnet Gravity, *Phys. Lett. B* **808**, 135658 (2020), [[arXiv:2003.11754](#)].
- [25] R. Kumar and S. G. Ghosh, Rotating black holes in 4D Einstein-Gauss-Bonnet gravity and its shadow, *JCAP* **07**, 053 (2020), [[arXiv:2003.08927](#)].
- [26] S. W. Wei and Y. X. Liu, Testing the nature of Gauss-Bonnet gravity by four-dimensional rotating black hole shadow, [arXiv:2003.07769](#).
- [27] R. A. Konoplya and A. Zhidenko, Simply rotating higher dimensional black holes in Einstein-Gauss-Bonnet theory, [arXiv:2007.10116](#).
- [28] S. G. Ghosh and S. D. Maharaj, Radiating black holes in the novel 4D Einstein-Gauss-Bonnet gravity, *Phys. Dark Univ.* **30**, 100687 (2020), [[arXiv:2003.09841](#)].
- [29] R. A. Konoplya and A. Zhidenko, (In)stability of black holes in the 4D Einstein-Gauss-Bonnet and Einstein-Lovelock gravities, *Phys. Dark Univ.* **30**, 100697 (2020), [[arXiv:2003.12492](#)].
- [30] S. A. Hosseini Mansoori, Thermodynamic geometry of the novel 4-D Gauss Bonnet AdS Black Hole, [arXiv:2003.13382](#).
- [31] S. W. Wei and Y. X. Liu, Extended thermodynamics and microstructures of four-dimensional charged Gauss-Bonnet black hole in AdS space, *Phys. Rev. D* **101**, 104018 (2020), [[arXiv:2003.14275](#)].
- [32] R. A. Konoplya and A. F. Zinhailo, Greybody factors and Hawking radiation of black holes in 4D Einstein-Gauss-Bonnet gravity, *Phys. Lett. B* **810**, 135793 (2020), [[arXiv:2004.02248](#)].
- [33] C. Y. Zhang, S. J. Zhang, P. C. Li and M. Guo, Superradiance and stability of the regularized 4D charged Einstein-Gauss-Bonnet black hole, [[arXiv:2004.03141](#)] [[gr-qc](#)]. *JHEP* **08**, 105 (2020), [[arXiv:2004.03141](#)].
- [34] A. Aragón, R. Bécar, P. A. González and Y. Vásquez, Perturbative and nonperturbative quasinormal modes of 4D Einstein-Gauss-Bonnet black holes, *Eur. Phys. J. C* **80**, 773 (2020), [[arXiv:2004.05632](#)].
- [35] P. Liu, C. Niu and C. Y. Zhang, Instability of the novel 4D charged Einstein-Gauss-Bonnet de-Sitter black hole, [arXiv:2004.10620](#).
- [36] S. U. Islam, R. Kumar and S. G. Ghosh, Gravitational lensing by black holes in the 4D Einstein-Gauss-Bonnet gravity, *JCAP* **09**, 030 (2020), [[arXiv:2004.01038](#)].
- [37] C. Liu, T. Zhu and Q. Wu, Thin Accretion Disk around a four-dimensional Einstein-Gauss-Bonnet Black Hole, [arXiv:2004.01662](#).
- [38] X. H. Ge and S. J. Sin, Causality of black holes in 4-dimensional Einstein-Gauss-Bonnet-Maxwell theory, *Eur. Phys. J. C* **80**, 695 (2020), [[arXiv:2004.12191](#)].
- [39] N. Dadhich, On causal structure of 4D-Einstein-Gauss-Bonnet black hole, *Eur. Phys. J. C* **80**, 832 (2020), [[arXiv:2005.05757](#)].
- [40] D. V. Singh, R. Kumar, S. G. Ghosh and S. D. Maharaj, Phase transition of AdS black holes in 4D EGB gravity coupled to nonlinear electrodynamics, [arXiv:2006.00594](#).
- [41] S. G. Ghosh, D. V. Singh and S. D. Maharaj, Regular black holes in Einstein-Gauss-Bonnet gravity, *Phys. Rev. D* **97**, 104050 (2018).
- [42] K. Jafarzade, M. Kord Zangeneh and F. S. N. Lobo, Optical features of AdS black holes in the novel 4D Einstein-Gauss-Bonnet gravity coupled to nonlinear electrodynamics, [arXiv:2009.12988](#).
- [43] K. Yang, B. M. Gu, S. W. Wei and Y. X. Liu, Born-Infeld black holes in 4D Einstein-Gauss-Bonnet gravity, *Eur. Phys. J. C* **80**, 662 (2020), [[arXiv:2004.14468](#)].
- [44] K. Jusufi, Nonlinear magnetically charged black holes in 4D Einstein-Gauss-Bonnet gravity, *Annals Phys.* **421**, 168285 (2020), [[arXiv:2005.00360](#)].
- [45] K. Akiyama et al., First M87 Event Horizon Telescope Results. I. The Shadow of the Supermassive Black Hole, *Astrophys. J.* **875**, L1 (2019), [[arXiv:1906.11238](#)].
- [46] K. Akiyama et al., First M87 Event Horizon Telescope Results. IV. Imaging the Central Supermassive Black Hole, *Astrophys. J.* **875**, L4 (2019), [[arXiv:1906.11241](#)].
- [47] M. Born and L. Infeld, Foundations of the new field theory, *Proc. R. Soc. Lond. A* **144**, 425 (1934).
- [48] E. S. Fradkin and A. A. Tseytlin, Effective field theory from quantized string, *Phys. Lett. B* **163**, 123 (1985).
- [49] R. R. Metsaev, M. A. Rakhmanov and A. A. Tseytlin, The Born-Infeld action as the effective action in the open superstring theory, *Phys. Lett. B* **193**, 207 (1987).
- [50] E. Bergshoeff, E. Sezgin, C. Pope and P. Townsend, The Born-Infeld action from conformal invariance of the open superstring, *Phys. Lett. B* **188**, 70 (1987).
- [51] D. L. Burke et al., Positron Production in Multiphoton Light-by-Light Scattering, *Phys. Rev. Lett.* **79**, 1626 (1997).
- [52] C. Bamber et al., Studies of nonlinear QED in collisions of 46.6-GeV electrons with intense laser pulses, *Phys. Rev. D* **60**, 092004 (1999).
- [53] D. Tommasini, A. Ferrando, H. Michinel and M. Seco, Detecting photon-photon scattering in vacuum at exawatt lasers, *Phys. Rev. A* **77**, 042101 (2008), [[arXiv:0802.0101](#)].
- [54] D. Tommasini, A. Ferrando, H. Michinel and M. Seco, Precision tests of QED and non-standard models by searching photon-photon scattering in vacuum with high

- power lasers, *J. High Energy Phys.* **0911**, 043 (2009), [[arXiv:0909.4663](#)].
- [55] O. J. Pike, F. Mackenroth, E. G. Hill and S. J. Rose, A photon–photon collider in a vacuum hohlraum, *Nature Photonics* **8**, 434 (2014).
- [56] Y. M. Xu, H. M. Wang, Y. X. Liu and S. W. Wei, Photon sphere and reentrant phase transition of charged Born-Infeld-AdS black holes, *Phys. Rev. D* **100**, 104044 (2019), [[arXiv:1906.03334](#)].
- [57] A. S. Habibina and H. S. Ramadhan, Geodesic of nonlinear electrodynamics and stable photon orbits, *Phys. Rev. D* **101**, 124036 (2020), [[arXiv:2007.03211](#)].
- [58] V. Perlick, O.Y. Tsupko and G.S. Bisnovaty-Kogan, Influence of a plasma on the shadow of a spherically symmetric black hole, *Phys. Rev. D* **92**, 104031 (2015), [[arXiv:1507.04217](#)].
- [59] S. W. Wei and Y. X. Liu, Observing the shadow of Einstein–Maxwell–Dilaton–Axion black hole, *JCAP* **11**, 063 (2013), [[arXiv:1311.4251](#)].
- [60] A. Belhaj, M. Benali, A. El Balali, H. El Moumni and S. E. Ennadifi, Deflection Angle and Shadow Behaviors of Quintessential Black Holes in arbitrary Dimensions, [[arXiv:2006.01078](#)].
- [61] A. Belhaj, M. Benali, A. El Balali, W. El Hadri and H. El Moumni, Shadows of Charged and Rotating Black Holes with a Cosmological Constant, [[arXiv:2007.09058](#)].
- [62] V. Cardoso, A. S. Miranda, E. Berti, H. Witek and V. T. Zanchin, Geodesic stability, Lyapunov exponents, and quasinormal modes, *Phys. Rev. D* **79**, 064016 (2009), [[arXiv:0812.1806](#)].
- [63] I. Z. Stefanov, S. S. Yazadjiev and G. G. Gylulchev, Connection between black-hole quasinormal modes and lensing in the strong deflection limit, *Phys. Rev. Lett.* **104**, 251103 (2010), [[arXiv:1003.1609](#)].
- [64] K. Jusufi, Quasinormal Modes of Black Holes Surrounded by Dark Matter and Their Connection with the Shadow Radius, *Phys. Rev. D* **101**, 084055 (2020), [[arXiv:1912.13320](#)].
- [65] K. Jusufi, Connection Between the Shadow Radius and Quasinormal Modes in Rotating Spacetimes, *Phys. Rev. D* **101**, 124063 (2020), [[arXiv:2004.04664](#)].
- [66] Y. Guo and Y. G. Miao, Null geodesics, quasinormal modes and the correspondence with shadows in high-dimensional Einstein-Yang-Mills spacetimes, [[arXiv:2007.08227](#)].
- [67] C. Lan, Y. G. Miao and H. Yang, Quasinormal Modes and Thermodynamics of Regular Black Holes, [[arXiv:2008.04609](#)].
- [68] S. W. Wei and Y. X. Liu, Null geodesics, Quasinormal modes, and thermodynamic phase transition for charged black holes in asymptotically flat and dS spacetimes, [[arXiv:1909.11911](#)].
- [69] S. Chandrasekhar, *The Mathematical Theory of Black Holes*, Oxford University Press, New York (1983).
- [70] S. Weinberg, *Gravitation and Cosmology: Principles and Applications of the General Theory of Relativity*, Wiley, New York (1972).
- [71] P. Kocherlakota and L. Rezzolla, Accurate mapping of spherically symmetric black holes in a parameterised framework, [[arXiv:2007.15593](#)].
- [72] W. Javed, J. Abbas and A. Övgün, Effect of the quintessential dark energy on weak deflection angle by Kerr-Newmann Black hole, [[arXiv:2007.16027](#)].
- [73] M. Zhang and R. B. Mann, Charged accelerating black hole in f(R) gravity, *Phys. Rev. D* **100**, 084061 (2019), [[arXiv:1908.05118](#)].
- [74] F. S. N. Lobo, A. Simpson and M. Visser, Dynamic thin-shell black-bounce traversable wormholes, *Phys. Rev. D* **101**, 124035 (2020), [[arXiv:2003.09419](#)].
- [75] T. Berry, F. S. N. Lobo, A. Simpson and M. Visser, Thin-shell traversable wormhole crafted from a regular black hole with asymptotically Minkowski core, *Phys. Rev. D* **102**, 064054 (2020), [[arXiv:2008.07046](#)].